Copy
RM L53G10b

NACA

RESEARCH MEMORANDUM

SOME FLUTTER EXPERIMENTS AT A MACH NUMBER OF 1.3 ON CANTILEVER WINGS WITH TUBULAR AND CLOSED BODIES AT THE TIPS

By John Locke McCarty and W. J. Tuovila

Langley Aeronautical Laboratory
Langley Field, Va.

NATIONAL ADVISORY COMMITTEE
FOR AERONAUTICS

WASHINGTON

October 7, 1953

NATIONAL ADVISORY COMMITTEE FOR AERONAUTICS

RESEARCH MEMORANDUM

SOME FLUTTER EXPERIMENTS AT A MACH NUMBER OF 1.3 ON CANTILEVER WINGS WITH TUBULAR AND CLOSED BODIES AT THE TIPS

By John Locke McCarty and W. J. Tuovila

SUMMARY

Flutter tests of 39 cantilever wings with tubular and closed bodies on the tips have been made in a small intermittent-flow supersonic wind tunnel where the testing technique involved changing the structural parameters so that the wing-body combinations would flutter at the tunnel Mach number of 1.3. Some effects of mass moment of inertia of the tube about the elastic axis, tube center-of-gravity location, and mass flow through the tube on the flutter-speed coefficient were studied. The experimental results are compared with a theory using two-dimensional air forces on the wing and tube forces derived from a modified slender-body theory.

The calculated flutter-speed coefficients are in reasonably good agreement with the experimental results except at bending to torsion frequency ratios near 1.0 where the calculated results are much lower than the experimental, and at frequency ratios greater than 1.3, where the calculated results are higher than the experimental. No real flutter-speed coefficients could be calculated for the configurations which consisted of wings and large closed bodies; however, calculated results were obtained for the very slender bodies, on which the body air forces were omitted. Divergence calculations were made for two wing-tube combinations and the results were unconservative by a wide margin.

INTRODUCTION

The aeroelastic phenomena of airplanes and missiles with ram-jet propulsion systems located at the wing tips may be influenced to a large extent by the flow through the propulsion unit. These effects have received little experimental or theoretical attention. Some theoretical work, however, has been done on the unsteady forces on slender bodies

which would be required in the analyses of these phenomena. Refs. 1 and 2, for instance, treat the problem of unsteady flow about slender closed bodies at supersonic speeds by means of linearized potential-flow theory. Some experimental results at subsonic speeds on the flutter of open and closed bodies mounted on slender struts are presented in reference 3. These results are compared with an analysis of the flutter and divergence of such bodies based on slender-body theory. No known experimental flutter data at supersonic speeds are available for wings with open or closed bodies mounted at the tips.

This paper presents the results of some tests on the flutter of cantilever wings at supersonic speed with tubular bodies, which simulate "cold" ram jets at the tips; the effect of internal air flow was investigated qualitatively by testing models with solid bodies of revolution and comparing the results with those obtained with tubular bodies having various amounts of internal flow. The tests were made in an intermittent-flow supersonic wind tunnel at a Mach number of 1.3. The experimental results are compared with those of an analytical development which considers two-dimensional supersonic wing forces and tube forces derived from slender-body theory.

SYMBOLS

b	root semichord, ft
f	flutter frequency, cps
f_h	first bending frequency, cps
f_α	first uncoupled torsion frequency, cps
g_h	first bending damping coefficient
g_α	first torsion damping coefficient
$(I_\alpha)_w$	mass moment of inertia of wing about elastic axis, slug-ft^2 per foot span
$(I_\alpha)_t$	mass moment of inertia of tube about elastic axis, slug-ft^2 per foot diameter
l	tube length, ft
l_w	wing length, in. (see fig. 1(a))

m_t average mass of tube, slugs per foot diameter

m_w mass of wing, slugs per foot span

$\left(r_\alpha^2\right)_t$ square of nondimensional radius of gyration of tube about elastic axis, $\frac{4(I_\alpha)_t}{m_t l^2}$

$\left(r_\alpha^2\right)_w$ square of nondimensional radius of gyration of wing about elastic axis, at root, $\frac{(I_\alpha)_w}{m_w b^2}$

R tube internal radius, in.

s elastic axis position in percent tube length, measured from leading edge of tube

t wing thickness, in.

V flutter speed, ft/sec

V_D divergence speed, ft/sec

x_o elastic-axis position in percent chord, measured from leading edge of wing

x_1 wing center-of-gravity position in percent chord, measured from leading edge of wing

z tube center-of-gravity position in percent tube length from elastic axis, measured positive behind elastic axis

$(1/\kappa)_t$ tube mass density ratio parameter, $\frac{4m_t}{\pi\rho l^2}$

$(1/\kappa)_w$ wing mass density ratio parameter at root, $\frac{m_w}{\pi\rho b^2}$

λ wing taper ratio, $\frac{\text{Tip chord}}{\text{Root chord}}$

ρ mass density of air in test section, slugs/cu ft

$\omega = 2\pi f$

$\omega_h = 2\pi f_h$

$\omega_\alpha = 2\pi f_\alpha$

$V/b\,\omega_\alpha$ flutter-speed coefficient

MODELS AND TEST METHODS

Models

The wings of the wing-tube combinations used in these flutter tests were made of either magnesium or wood. All magnesium wings were rectangular in plan form with a chord of 3 inches and a thickness of 0.064 inch with the exception of one wing which was 0.033 inch thick. The wooden wings were constructed of spruce or birch, laminated or nonlaminated, with both rectangular and tapered plan forms; the rectangular wings had chords of approximately 2.50 inches, and the tapered wings had a taper ratio ranging from 0.373 to 0.502, with a root chord ranging from 2.85 to 3.00 inches. All wings were of constant thickness and were hexagonal in cross section (see fig. 1(a)).

Balsa-wood tubes of 1/16-inch wall thickness coated with glass cloth and aluminum tubes of 0.005-0.010-inch wall thickness were mounted at the tips of the various wings. A general description of the wing-tube combinations is given in the sketch in figure 1(a). This figure illustrates the manner in which the tubes were mounted on the wing. The wings were extended through the tubes to provide a rigid connection between the two, but the wing tips were considered to be located where the wings entered the tubes. Strips of lead were taped to the tube to change the mass and inertia of the tube or to give a desired center-of-gravity location.

The tubes in general were 7 inches in length with an inside diameter of 1 inch. Three of the tubes from which flutter data were obtained, however, were 0.75 inch in diameter and others were less than 7 inches in length.

Diffuser cones of various sizes and shapes, as illustrated in figure 1(b), were installed in the noses of 8 tubes in order to investigate the effects of inlet shape and mass flow through the tube on the flutter-speed coefficient. Flutter data were also obtained from three closed bodies of revolution, 0.55-inch maximum outside radius, simulating external stores on wing tips (see fig. 1(c)) and from two very slender bodies of total mass and inertia equivalent to the tubes (see fig. 1(d)).

Some of the geometric, inertial, and structural properties of the combinations are listed in table 1. Included in table 1 are the first bending mode frequencies and the first torsional mode frequencies. The first bending mode frequency was taken as the coupled first bending mode frequency, which was obtained by exciting the wing at the elastic axis and recording the oscillations. The first torsional mode frequency was determined by exciting the model in torsion while supporting the wing tip at the elastic axis. Structural damping values were obtained from oscillograph records of both frequencies.

Test Methods

The models were mounted at zero angle of attack as cantilevers on an injector and were tested at a Mach number of 1.3 in an intermittent-flow supersonic wind tunnel having a 9- by 18-inch test section. The testing technique involved injecting the models into and retracting them from the tunnel while the flow was steady at a Mach number of 1.3. This technique was used to avoid any possible flutter that might occur during the tunnel starting and stopping transients. The testing procedure was to clamp the wing very short to be sure the wing-tube combination would not flutter and then to increase the span in successive tunnel runs until flutter occurred. If flutter had not occurred when the wing length reached 4 inches, the structural parameters or the location of the tube center of gravity were changed rather than further extending the wing in order to avoid possible interference effects from the opposite wall of the tunnel.

Most of the structural-parameter changes were brought about by reducing the root thickness in order to change the bending stiffness, or by slitting the leading and trailing edges at the root, in order to change the torsional stiffness. The center of gravity of the tube was shifted by taping lead strips to the tube. Structural-parameter changes or changes in the center of gravity were continued until the combination fluttered. A more detailed description of the test methods and photographs of the apparatus can be found in reference 4.

The root strains, position of the model in the tunnel, and the static pressure in the test section were recorded simultaneously by a recording oscillograph.

METHOD OF ANALYSIS

In the method of analysis employed in this paper two-dimensional supersonic air force coefficients from reference 5 were used for the

wings, and the aerodynamic forces given in the appendix of reference 3 were used for the tubes and closed bodies of revolution.

In calculating the flutter-speed coefficients of the combinations, use was made of the ratio of the experimental first natural bending frequency to the torsion frequency and of the measured first bending and first torsion damping coefficients. For combinations having rectangular wings, linear torsion and parabolic bending mode shapes were assumed, and for the combinations having tapered wings the calculated natural mode shapes were used. The 70-percent-span station was taken as representative of the entire wing on all models except for some tapered wings having high ratios of bending to torsion frequency, where it was necessary to integrate the wing parameters along the span in order to obtain a flutter solution.

Figure 2 shows the relationship between the theoretical flutter-speed coefficients, $V/b\omega_\alpha$ obtained from both a spanwise-integration and a representative-section analysis and the ratio of first natural bending to torsion frequency ω_h/ω_α for the tapered wing model 20. The two methods of calculation are in good agreement and it may be noted that the spanwise-integration method serves to extend the flutter solution to a slightly higher ratio of natural bending to torsion frequency, in the sense that it predicts flutter for values of this ratio at which the other method no longer predicts flutter (at least in the first mode).

The aerodynamic forces on the tubes and bodies were based upon a modified slender-body theory as in reference 3. This modified theory disregards the concentrated forces on the tail section of the tube on the premise that both the external and internal flows leave the trailing edge of the tube tangentially and are not realined with the free stream. The calculations of the flutter-speed coefficients for combinations having a diffuser cone did not consider the aerodynamics of the cone, and were based on the assumption that the cone did not impede the flow through the tube. For the calculations of the two combinations having very slender bodies, the body air forces were omitted.

The divergence velocities were calculated for two wing-tube combinations by equating the aerodynamic moment on the tube (for $\omega = 0$), as taken from reference 3, to the restoring moment applied to the tube by the wing. Since the elastic axis on all models was at the midchord of the wing and since the linearized two-dimensional supersonic theory predicts zero moment about the midchord for these wings, only the tubes contributed to the moment in these calculations.

RESULTS AND DISCUSSION

Presentation of Data

All combinations from which either flutter or divergence data were obtained are listed in table 1. This table is divided for convenience into four sections: flutter of open tubes, flutter of tubes with diffuser cones, flutter of closed bodies, and divergence of open tubes. In the table are listed the significant properties of the combinations and the experimental and analytical results.

Experimental Results

As previously mentioned, the tunnel conditions were fixed and it was necessary to change the properties of the combinations to obtain flutter. Inasmuch as it is generally difficult in experiments to change one parameter without changing others, it is difficult to obtain the effect of variations in a single parameter on the quantity of interest, in this instance, the flutter-speed coefficient. Consequently, in the following paragraphs the effects of various parameters are discussed on the basis of a comparison of those combinations which varied in essentially only one parameter. In this way, the effect of wing taper ratio, tube inertia, mass flow through the tube, and center-of-gravity location on the flutter-speed coefficient could be noted, although some of the conclusions had to be based on comparisons of only two combinations. It should be noted that in all of these tests the flutter speed and the tube length were constants, so that changes in the flutter-speed coefficient reflect changes in the torsional frequency which caused the given combination to flutter.

Tube inertia.- The results for combinations 13 and 14 indicate that the flutter-speed coefficient increases with increased mass moment of inertia of the tube about the elastic axis. In other words, although increasing the mass moment of inertia of the tube actually would tend to decrease the flutter speed as a result of the reduced torsional frequency, the decrease in the flutter speed is apparently less than that in the torsional frequency, so that the flutter-speed coefficient is increased.

Mass flow through tube.- Results for combinations 13 and 30, 27 and 7, and 26 and 6 indicate that the flutter-speed coefficient increases with decreasing mass flow through the tube; eliminating the internal flow entirely increases the flutter-speed coefficient further as shown by the results for combinations 37 and 22, 36 and 14, and 35 and 19.

Center-of-gravity location.- The effect of the center-of-gravity location on the flutter-speed coefficient was observed directly since the flutter condition in some cases was approached by shifting the center of gravity of the tube rearward. Thus the flutter-speed coefficient is increased by moving the center of gravity of the tube forward.

Frequency ratio.- No direct experimental relationship between the frequency ratio and the flutter-speed coefficient can be obtained from a comparison of combinations listed in table 1. The theoretical variation of the flutter-speed coefficient with frequency ratio is, however, illustrated in figure 2 for one of the combinations tested. This figure is typical of combinations presented in this report.

It may be seen that the flutter-speed coefficient decreases to a minimum value at a frequency ratio near 1.0 and increases rapidly thereafter with an increase in frequency ratio. A comparison of figures 2 and 3 indicates that the experiments follow a similar trend, but the decrease in the experimental flutter-speed coefficient in the frequency ratio region of 1.0 is less pronounced than that indicated by the curve of calculated flutter-speed coefficients. In fact, the experimental flutter-speed coefficient is almost independent of the bending to torsion frequency ratio.

Divergence.- Wing-tube combinations 38 and 39 diverged before a flutter condition could be reached because their forward center-of-gravity location tended to increase the flutter-speed coefficient, whereas the forward tube location and the thick wings tended to decrease the divergence speed.

Comparison of Theory With Experiment

Flutter calculations were made for all combinations which fluttered. Solutions were obtained for the wing-tube combinations and also for the combinations of wings and the very slender bodies on which the air forces were neglected. No solutions could be obtained, however, for the combinations of wings and the closed bodies on which the body air forces were included. These results indicate that the air forces used on the closed bodies are stabilizing inasmuch as these wing—closed-body combinations appear to be stable theoretically.

Flutter-speed coefficient.- A comparison of the calculated and experimental results on the basis of the flutter-speed coefficient $V/b\omega_\alpha$ is made in figure 3. In this figure, the ratio of the experimental flutter-speed coefficient to the theoretical flutter-speed coefficient is plotted against the ratio of first natural bending to torsion frequency ω_h/ω_α. In the lower range of this ratio the calcu-

lated flutter-speed coefficient is within 20 percent of the experimental flutter-speed coefficient. When the natural frequency ratio is near 1.0, however, the experimental flutter-speed coefficient tends to be much higher than the calculated flutter-speed coefficient. In the natural frequency ratio region of 1.2 the measured flutter-speed coefficient again agrees with the calculated flutter-speed coefficient, but as the natural frequency ratio increases beyond 1.3 the measured flutter-speed coefficient becomes less than the calculated; in other words, the calculations become unconservative.

The deviations may be explained by an examination of the theoretical flutter curve as presented in figure 2, which indicates a type of resonant condition near the frequency ratio of 1.0 and an asymptotic behavior at ratios greater than 1.2. (For other combinations the asymptotic tendency occurs at other frequency ratios.) As stated previously, the experimental flutter-speed coefficient is almost independent of the ratio of bending to torsion frequency; the experimental flutter-speed coefficients tend to be lower when the ratio ω_h/ω_α is near 1.0 than elsewhere, and they tend to increase as this ratio increases beyond 1.0, but these variations are much less pronounced than those of the calculated flutter-speed coefficients. Therefore, the variation of the ratio of experimental to calculated flutter-speed coefficient in figure 3 is primarily due to the variation in the calculated flutter-speed coefficient. In general, considering slight experimental errors and the fact that wing aspect ratio, tube inlet shape, tube mass flow, and interference effects were neglected in the theoretical analysis, the agreement between the calculations and the experiment for tubes is satisfactory except for the regions where ω_h/ω_α equals 1.0 and where ω_h/ω_α is greater than 1.3.

Flutter frequency.- Figure 4 is a plot of the ratio of the experimentally obtained ratio ω/ω_α to the calculated ratio ω/ω_α against the ratio of the natural bending to torsion frequencies. This figure indicates that the theory predicts the flutter frequency reasonably well.

Divergence.- Divergence calculations were made by using the formula in reference 3 and the results are very unconservative; the actual divergence speed being 1430 feet per second, whereas the calculated divergence speeds are 2140 and 2470 feet per second for combinations 38 and 39, respectively. Apparently, the divergence calculations greatly underestimate the aerodynamic moment. This discrepancy may be due to two reasons. The assumed flow conditions at the tail section may be unrealistic and large forces may exist there. Also, the chordwise center of pressure of the steady aerodynamic forces on the wing, as given by linearized theory, is at the midchord but is known to be actually ahead of the midchord position, giving an additional moment not included in the analysis.

CONCLUDING REMARKS

Flutter tests of 39 cantilever wings with tubular and closed bodies on the tips were made in a small intermittent-flow supersonic wind tunnel where the testing technique involved changing the structural parameters so that the wing-body combinations would flutter at the tunnel Mach number of 1.3. The following conclusions were made:

1. The experimental results indicate that within the range of model parameters the flutter-speed coefficient is increased (other parameters remaining fixed) by increasing the mass moment of inertia of the tube about the elastic axis, shifting the center of gravity of the tube forward, and decreasing the mass flow of air through the tube.

2. The calculated flutter-speed coefficients are in reasonably good agreement with the experimental results except at ratios of bending to torsion frequency near 1.0 where the results of the calculations tend to be conservative by a wide margin and at ratios of bending to torsion frequency greater than about 1.3 and up to the highest natural frequency ratio of 1.43 where the results of the calculations tend to be somewhat unconservative.

3. A plot of the calculated flutter-speed coefficient against the ratio of bending to torsion frequency indicates a minimum flutter-speed coefficient near the frequency ratio of 1.0 and thereafter a very rapid increase with increased frequency ratio. It appears, therefore, that the experimental variation of the flutter-speed coefficient with the natural frequency ratio is similar to the calculated but not as pronounced.

4. No real flutter-speed coefficients could be calculated for the combinations of wings and closed bodies; however, calculated results were obtained for the very slender bodies on which the body air forces were omitted.

5. The calculated flutter frequencies are in good agreement with the experimental flutter frequencies.

6. Two wing-tube combinations diverged before a flutter condition could be reached. The results of divergence calculations based on linearized two-dimensional theory were unconservative by a wide margin for these two cases.

Langley Aeronautical Laboratory,
National Advisory Committee for Aeronautics,
Langley Field, Va., August 6, 1953.

REFERENCES

1. Stewartson, K.: On Linearized Potential Theory of Unsteady Supersonic Motion. Quarterly Jour. Mech. and Applied Math., vol. III, pt. 2, June 1950, pp. 182-199.

2. Miles, John W.: On Non-Steady Motion of Slender Bodies. Aeronautical Quarterly, vol. II, pt. III, Nov. 1950, pp. 183-194.

3. Clevenson, S. A., Widmayer, E., Jr., and Diederich, Franklin W.: An Exploratory Investigation of Some Types of Aeroelastic Instability of Open and Closed Bodies of Revolution Mounted on Slender Struts. NACA RM L53E07, 1953.

4. Tuovila, W. J., Baker, John E., and Regier, Arthur A.: Initial Experiments on Flutter of Unswept Cantilever Wings at Mach Number 1.3. NACA RM L8J11, 1949.

5. Garrick, I. E., and Rubinow, S. I.: Flutter and Oscillating Air-Force Calculations for an Airfoil in a Two-Dimensional Supersonic Flow. NACA Rep. 846, 1946. (Supersedes NACA TN 1158.)

TABLE I.- MODEL PARAMETERS AND RESULTS

$[x_0 = 0.50;\ x_1 = 0.50;\ \rho = 0.00090]$

Model	Parameter																								
	Wing material	λ	t	l_w	Aspect ratio	Tube material	R	s	z	Cone	$(1/\kappa)_w$	$(1/\kappa)_t$	$(r_\alpha^2)_w$	$(r_\alpha^2)_t$	b	f_h	f_α	f	g_h	g_α	I	ω_h/ω_α	$(V/b\omega_\alpha)_{exp}$	$(V/b\omega_\alpha)_{calc}$	$(\omega/\omega_\alpha)_{exp}$	$(\omega/\omega_\alpha)_{calc}$	$(V_D)_{calc}$
Flutter of open tubes																											
1	magnesium	1.0	0.064	3.875	2.58	aluminum	0.50	42.86	2.043		95.7	36.1	0.262	0.212	0.125	60	145	73	0.010	(a)	0.583	0.414	12.55	13.82	0.503	0.727	
2	magnesium	1.0	0.064	3.438	2.29	balsa	0.50	50.00	0		95.7	28.5	0.262	0.215	0.125	70	162	100	0.015	(a)	0.583	0.432	11.24	9.30	0.617	0.660	
3	wood	1.0	0.180	4.25	3.40	balsa	0.50	42.86	4.286		129.5	54.6	0.188	0.287	0.104	49.5	109	72	0.017	0.020	0.583	0.454	20.08	18.36	0.661	0.729	
4	magnesium	1.0	0.064	2.875	1.92	aluminum	0.50	43.64	1.658		95.7	39.9	0.262	0.232	0.125	80	165	105	0.010	(a)	0.573	0.485	11.04	13.06	0.636	0.741	
5	magnesium	1.0	0.064	3.5	2.33	aluminum	0.50	42.86	-0.957		95.7	77.1	0.262	0.372	0.125	48	93	60	0.014	0.010	0.583	0.516	19.60	24.39	0.645	0.813	
6	magnesium	1.0	0.064	2.5	1.67	aluminum	0.50	42.86	5.243		95.7	65.5	0.262	0.288	0.125	77	140	97	0.008	(a)	0.583	0.550	13.02	15.01	0.693	0.795	
7	magnesium	1.0	0.064	2.0	1.33	aluminum	0.50	42.86	12.443		95.7	77.1	0.262	0.403	0.125	91	142	100	0.005	0.001	0.583	0.641	12.83	16.40	0.704	0.870	
8	magnesium	1.0	0.033	1.125	0.75	aluminum	0.50	50.00	0		42.3	49.7	0.308	0.353	0.125	75	106	85	0.019	0.031	0.583	0.708	17.20	16.30	0.802	0.820	
9	wood	1.0	0.190	4.0	3.20	balsa	0.50	42.86	4.286		85.3	67.3	0.230	0.411	0.104	70.5	92	75	0.010	0.018	0.583	0.766	23.79	14.16	0.815	0.883	
10	magnesium	1.0	0.064	1.656	1.10	aluminum	0.50	42.86	5.543		95.7	115.3	0.262	0.438	0.125	89	116	100	0.010	(a)	0.583	0.767	15.71	18.70	0.862	0.917	
11	magnesium	1.0	0.064	1.25	0.833	aluminum	0.50	43.64	3.360		95.7	66.7	0.262	0.483	0.125	144	159	145	0.031	(a)	0.573	0.906	11.45	12.95	0.912	0.976	
12	magnesium	1.0	0.064	1.5	1.00	balsa	0.50	50.00	6.00		95.7	48.8	0.262	0.439	0.125	145	[b]147	140	0.003	0.003	0.583	0.987	12.67	12.84	0.952	0.996	
13	wood	1.0	0.150	3.0	2.40	balsa	0.50	42.86	4.286		109.7	67.3	0.187	0.345	0.104	108	108	98	0.029	0.034	0.583	1.00	20.26	11.64	0.907	0.993	
14	wood	1.0	0.165	3.4375	2.75	balsa	0.50	42.86	4.286		74.12	67.3	0.206	0.435	0.104	87	87	80	0.030	0.038	0.583	1.00	25.15	9.95	0.920	1.00	
15	wood	0.450	0.156	4.00	3.38	balsa	0.375	42.86	4.286		67.9	86.6	0.240	0.537	0.122	58	54	48	0.018	0.026	0.583	1.074	34.53	13.38	0.889	1.02	
16	wood	1.0	0.180	4.00	3.225	balsa	0.375	42.86	4.286		64.7	86.6	0.264	0.533	0.103	67	59	63	0.015	0.021	0.583	1.135	37.44	37.44	1.068	1.075	
17	wood	0.44	0.188	4.00	3.70	balsa	0.50	42.86	4.286		79.8	54.6	0.225	0.409	0.125	92	81	82	0.019	0.026	0.583	1.136	22.47	15.60	1.012	1.071	
18	wood	0.373	0.170	4.00	3.88	balsa	0.50	42.86	4.286		63.5	67.3	0.243	0.466	0.125	68	57	59	0.017	0.027	0.583	1.193	31.95	34.05	1.035	1.070	
19	wood	0.373	0.200	4.00	3.95	balsa	0.50	43.23	4.323		78.6	55.5	0.244	0.419	0.123	119	98	105	0.011	0.023	0.578	1.214	18.87	17.98	1.071	1.163	
20	wood	0.471	0.125	3.75	3.50	balsa	0.50	42.86	4.286		68.3	67.3	0.240	0.458	0.121	75	61	68	0.013	0.023	0.583	1.230	30.82	33.98	1.115	1.099	
21	wood	0.450	0.180	4.00	3.76	balsa	0.375	42.86	4.286		65.1	86.6	0.241	0.540	0.122	63	49	53	0.014	0.025	0.583	1.286	38.06	47.80	1.082	1.083	
22	wood	0.502	0.125	4.00	3.45	balsa	0.50	42.86	4.357		65.4	71.5	0.244	0.464	0.129	81.5	59.5	71	0.013	0.025	0.583	1.370	29.63	103.90	1.193	1.124	
23	wood	0.450	0.188	4.00	3.74	balsa	0.50	46.296	3.086		70.7	127.3	0.243	0.295	0.123	69	50	62	0.017	0.072	0.540	1.380	37.00	66.75	1.240	1.010	
24	wood	0.383	0.180	4.00	4.07	balsa	0.50	42.86	4.286		69.3	54.6	0.245	0.415	0.119	89.5	62.5	77	0.011	0.032	0.583	1.432	30.60	69.10	1.232	1.191	
Flutter of tubes with diffuser cones																											
25	magnesium	1.00	0.064	3.50	2.33	aluminum	0.50	43.64	0.160	1	95.7	41.2	0.262	0.250	0.125	59	140	87	0.013	(a)	0.573	0.421	13.01	13.00	0.621	0.669	
26	magnesium	1.00	0.064	3.25	2.17	aluminum	0.50	42.86	3.943	2	95.7	70.4	0.262	0.319	0.125	55	104	63	0.014	(a)	0.583	0.529	17.50	15.14	0.606	0.818	
27	magnesium	1.00	0.064	2.50	1.67	aluminum	0.50	42.86	10.643	2	95.7	81.9	0.262	0.378	0.125	70	101	75	0.011	(a)	0.583	0.693	18.03	14.98	0.743	0.871	
28	magnesium	1.00	0.064	1.594	1.06	aluminum	0.50	42.86	6.143	1	95.7	118.3	0.262	0.454	0.125	96	117	104	0.005	0.005	0.583	0.821	15.56	15.56	0.889	0.922	
29	wood	0.443	0.200	4.00	3.69	balsa	0.50	42.86	4.286	4	78.6	67.3	0.244	0.490	0.125	68	68	62	0.017	0.022	0.583	1.00	26.77	11.66	0.912	1.002	
30	wood	1.00	0.180	3.4375	2.75	balsa	0.50	42.86	4.286	3	74.1	67.3	0.245	0.360	0.104	92	91	80	0.028	0.031	0.583	1.011	24.04	14.02	0.879	1.023	
31	wood	1.00	0.150	2.875	2.33	balsa	0.50	42.86	4.286	4	112.4	67.3	0.209	0.383	0.103	114	104	105	0.029	0.051	0.583	1.096	21.23	14.86	1.010	1.064	
32	wood	1.00	0.200	4.00	3.20	balsa	0.50	42.86	4.286	4	85.4	67.3	0.219	0.436	0.104	110	90	92	0.016	0.033	0.583	1.222	24.31	26.08	1.022	1.114	
Flutter of closed bodies																											
33	wood	1.00	0.188	4.00	3.20	body		45.35	4.00		86.1	56.8	0.230	0.318	0.104	110	90	(c)	0.015	0.028	0.625	1.222	24.32				
34	wood	1.00	0.188	4.00	3.20	body		48.57	4.286		86.1	65.2	0.230	0.357	0.104	108	86	88	0.014	0.032	0.583	1.256	25.42		1.023		
35	wood	0.50	0.188	4.00	3.56	body		45.37	4.00		73.7	56.2	0.243	0.345	0.125	87	72	72	0.013	0.019	0.625	1.208	25.28		1.00		
36	wood	1.00	0.125	3.625	2.90	very slender body		44.93	5.084		86.1	304.4	0.230	0.383	0.104	84	83	80	0.024	0.023	0.492	1.012	26.34	9.95	0.964	0.985	
37	wood	0.52	0.188	4.00	3.51	very slender body		44.93	5.084		73.7	307.2	0.243	0.421	0.125	68	53	65	0.014	0.011	0.492	1.283	34.36	42.23	1.226	1.047	
Divergence of open tubes																											
38	wood	1.00	0.188	4.50	3.60	balsa	0.50	50.0	0.247		80.7	39.2	0.233	0.307	0.104	108	112		0.007	0.020	0.583	0.964	[d]19.54	10.65		0.980	2140
39	wood	1.00	0.155	3.25	2.60	balsa	0.50	50.0	0		59.9	56.2	0.255	0.307	0.104	129	108		0.013	0.023	0.583	1.194	[d]20.27	61.10		1.130	2470

[a] 0.0050 assumed for theoretical calculations.

[b] Calculated.

[c] Not obtained.

[d] V = Divergence velocity.

NACA

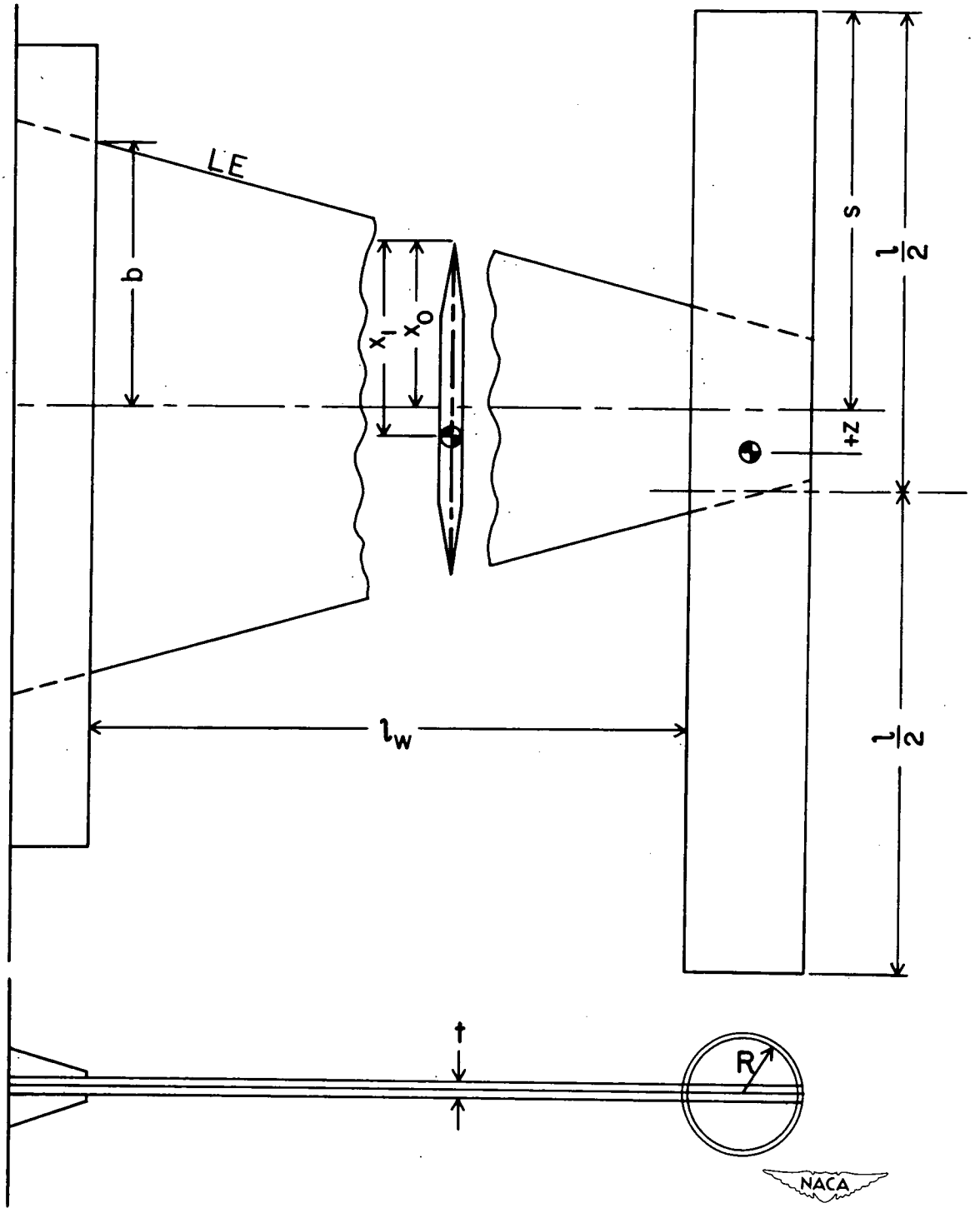

(a) Wing-tube combination.

Figure 1.- Sketches of combinations.

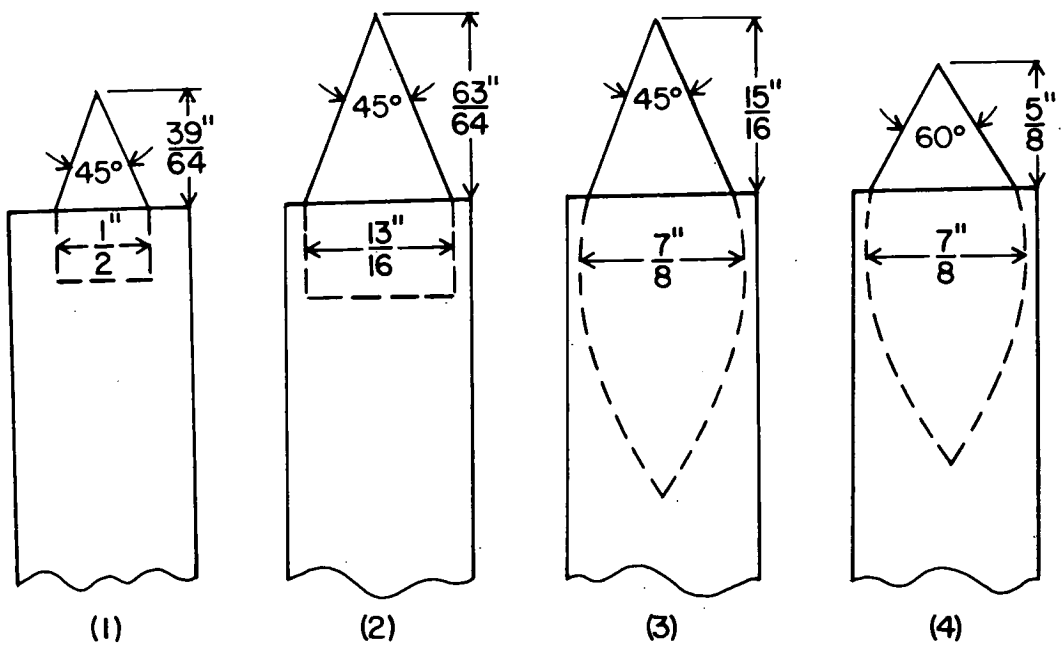

(b) Diffuser cones.

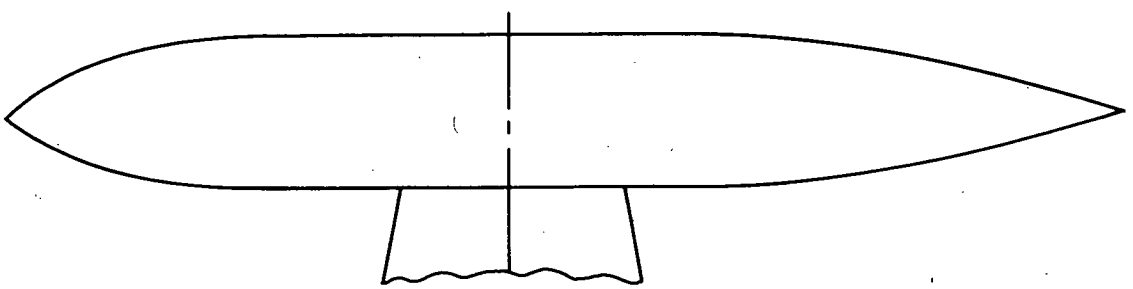

(c) Closed body.

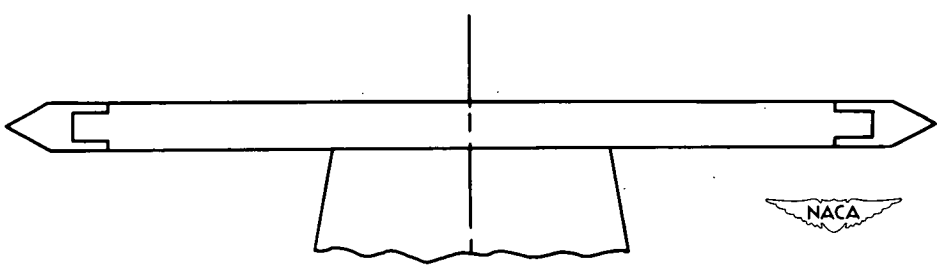

(d) Very slender body.

Figure 1.- Concluded.

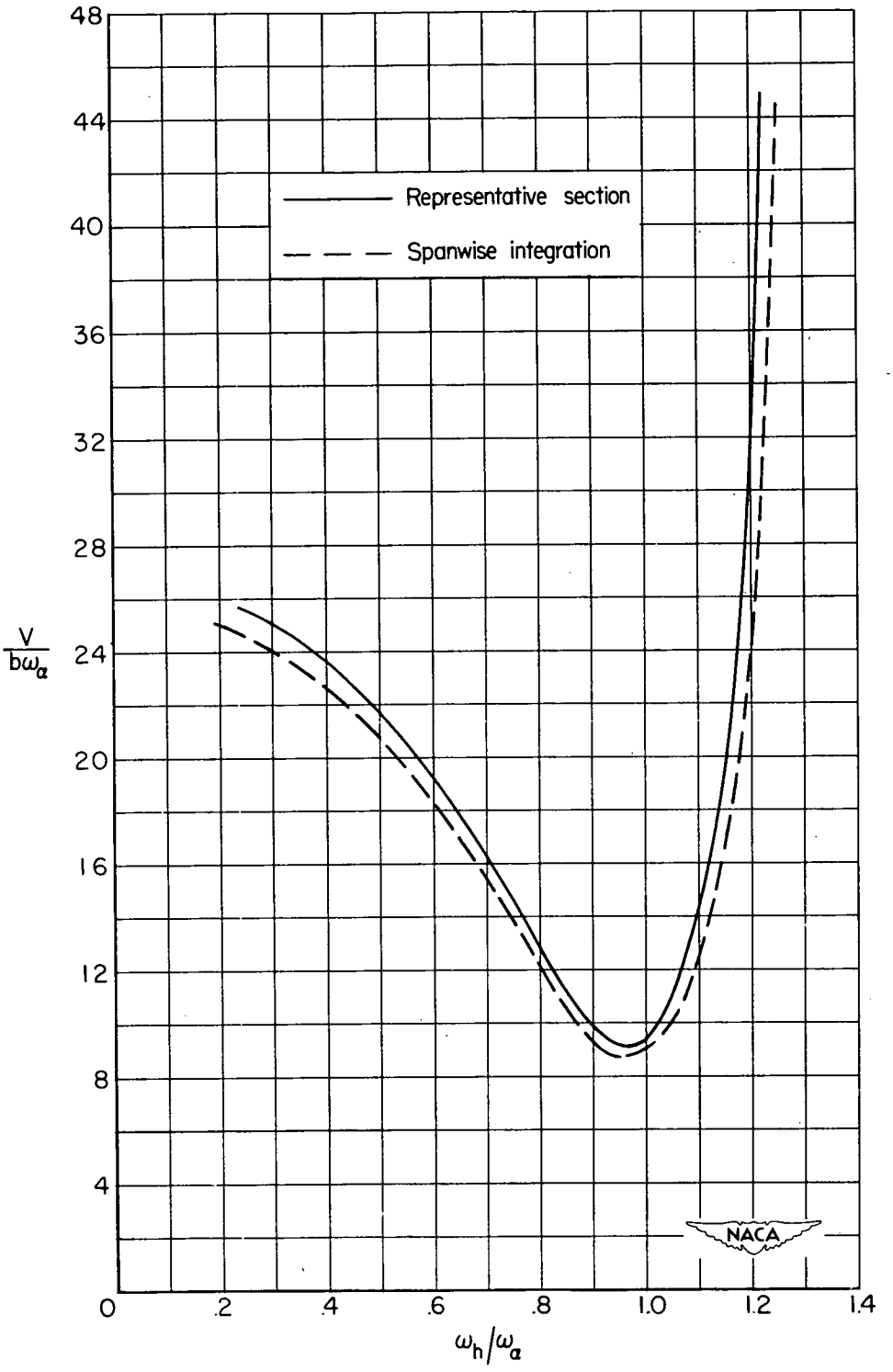

Figure 2.- Calculated flutter-speed coefficient plotted against ratio of natural bending to torsion frequency for model 20; both the representative-section and spanwise-integration analyses are illustrated.

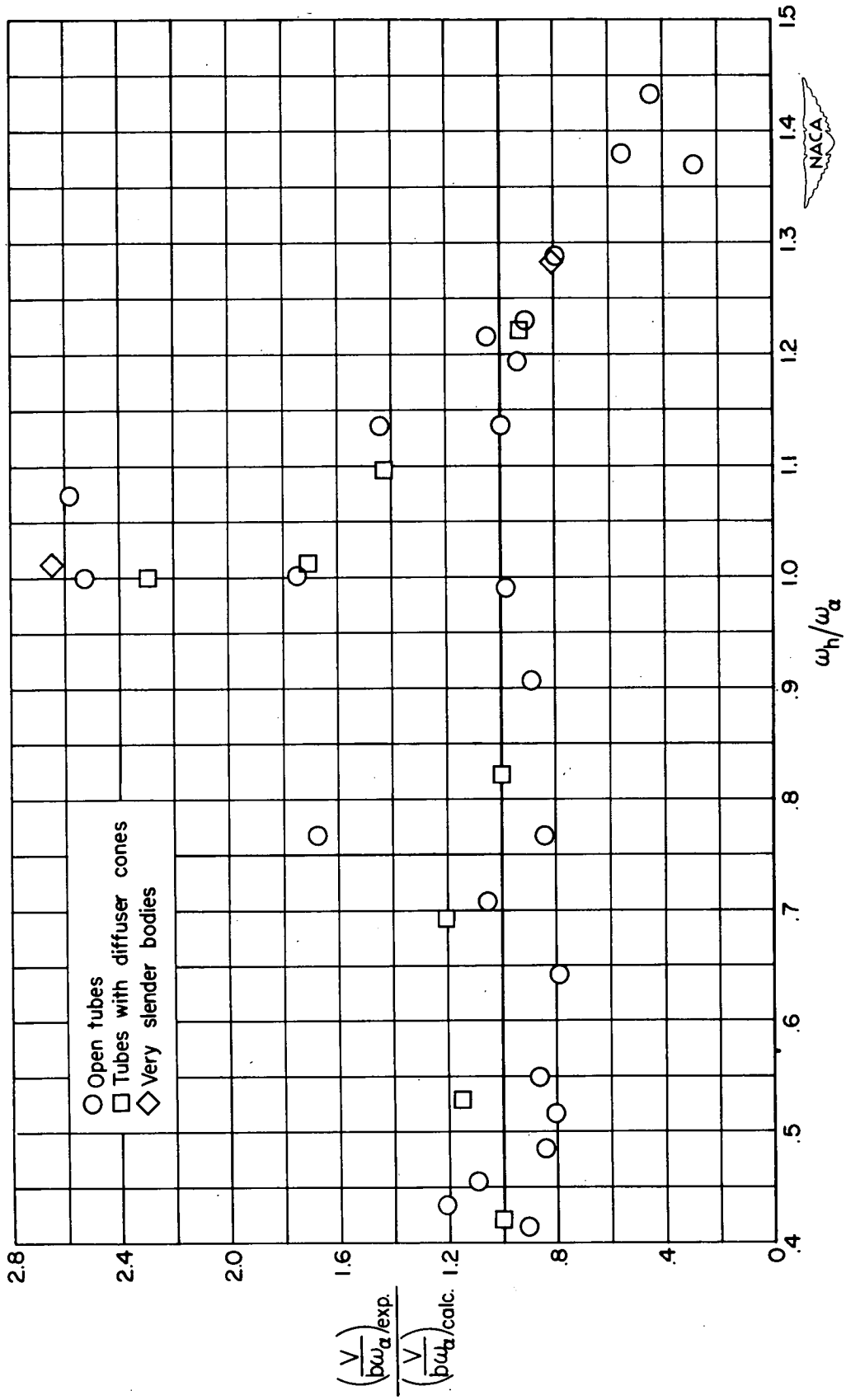

Figure 3.- Ratio of experimental to calculated flutter-speed coefficient plotted against ratio of natural bending to torsion frequency.

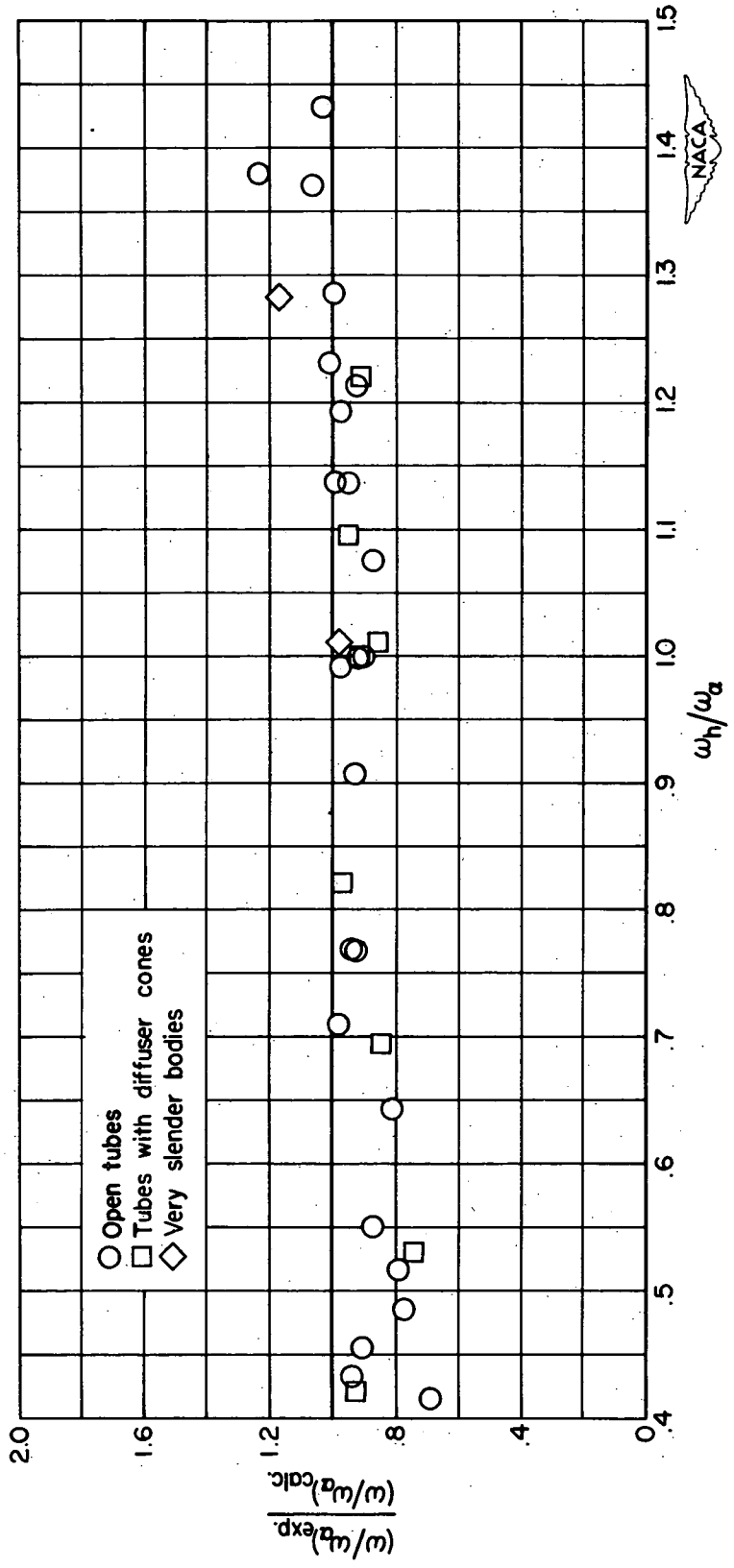

Figure 4.- Ratio of experimental to calculated ω/ω_α plotted against ratio of natural bending to torsion frequency.